ISPRS Journal of Photogrammetry and Remote Sensing xxx (xxxx) xxx–xxx

Contents lists available at ScienceDirect

ISPRS Journal of Photogrammetry and Remote Sensing

journal homepage: www.elsevier.com/locate/isprsjprs

# An analytical approach to evaluate point cloud registration error utilizing targets

Ronghua Yang[a,b,c,*], Xiaolin Meng[d], Yibin Yao[e], Bi Yu Chen[f], Yangsheng You[a,b], Zejun Xiang[c]

[a] Key Laboratory of New Technology for Construction of Cities in Mountain Area (Chongqing University), Ministry of Education, Chongqing 400045, China
[b] School of Civil Engineering, Chongqing University, Chongqing 400045, China
[c] Chongqing Survey Institute, Chongqing 401121, China
[d] Nottingham Geospatial Institute, The University of Nottingham, Nottingham NG7 2TU, UK
[e] School of Geodesy and Geomatics, Wuhan University, Wuhan 430079, China
[f] State Key Laboratory of Information Engineering in Surveying, Mapping and Remote Sensing, Wuhan University, Wuhan 430079, China

ARTICLE INFO

*Keywords:*
Point cloud
Registration error
Target
Terrestrial laser scanning

ABSTRACT

Point cloud registration is essential for processing terrestrial laser scanning (TLS) point cloud datasets. The registration precision directly influences and determines the practical usefulness of TLS surveys. However, in terms of target based registration, analytical point cloud registration error models employed by scanner manufactures are only suitable to evaluate target registration error, rather than point cloud registration error. This paper proposes an new analytical approach called the registration error (***RE***) model to directly evaluate point cloud registration error. We verify the proposed model by comparing ***RE*** and root mean square error (***RMSE***) for all points in three point clouds that are approximately equivalent.

## 1. Introduction

Terrestrial laser scanning (TLS) is used for a rapid collection of dense, three-dimensional (3D) spatial point cloud datasets of an entire object. Usually several scans are required with different stations to survey a relatively large and complex object completely due to occluded surfaces and scanner field of view limitations (Reshetyuk, 2009). To obtain the object's complete 3D model, the point cloud datasets must first be registered to a chosen coordinate system (Zhang, 2012).

Previous registration studies mainly include: (1) Matric representation for rotation transformation, such as Euler angle (Lichti and Skaloud, 2010; Zhang, 2008), unit quaternion (Lichti and Skaloud, 2010; Zhang, 2008; Yang, 2011), direction cosines (Lichti and Skaloud, 2010; Yang, 2011), dual quaternions (Walker and Shao, 1991), etc.; (2) Algorithms to compute 3-D rigid body transformation, such as singular value decomposition (Eggert et al., 1997; Arun et al., 1987), unit quaternion (Eggert et al., 1997; Faugeras and Hebert, 1986; Horn, 1987), dual quaternions (Walker and Shao, 1991; Eggert et al., 1997), orthonormal matric (Eggert et al., 1997; Horn et al., 1988), Lodrigues matric (Yao et al., 2007), etc.; (3) Iterative closest point method (ICP) (and variants), such as the feature correspondences (Salvi et al., 2007; Besl and Mckay, 1992; Tarel et al., 1998; Stamos and Leordeanu, 2003), registration strategy (Salvi et al., 2007; Chuang et al., 1998; Carmichael et al., 1999), correspondence search (Salvi et al., 2007; Chow et al., 2004; Zinsser et al, 2003), robustness (Salvi et al., 2007; Chow et al., 2004; Zinsser et al, 2003), etc.; (4) Point cloud registration error models, such as error propagation for two scans (Wang, 2006), error propagation for multiple scans (Zhang, 2012; Wang, 2006; Sharp et al., 2004), directly geo-referenced TLS data precision (Lichti et al., 2005; Fan et al., 2015), the relationship between target precision and distribution relationships (Reshetyuk, 2009; Gordon and Lichti, 2004; Harvey, 2004; Bornaz et al., 2003), etc.

For target registration, point cloud registration error models and their statistics employed by scanner manufacturer software are based on how well the targets match. These approaches have been shown to be inadequate (Fan et al., 2015), since target registration error is not equal to the point cloud registration error. Although Fan et al. (2015) recommended a model to evaluate registration error based on how well the point clouds matched, However, the model was derived from simulations, which are not always consistent with actual outcomes since practical situations are often very complicated. Therefore, this paper derives the target based point cloud registration error model analytically, and verifies the model by evaluating real-world point cloud registration precision.

## 2. Estimation of registration parameters

We first introduce the common registration model to provide true

* Corresponding author at: Key Laboratory of New Technology for Construction of Cities in Mountain Area (Chongqing University), Ministry of Education, Chongqing 400045, China.
*E-mail address:* rh_yang@cqu.edu.cn (R. Yang).

https://doi.org/10.1016/j.isprsjprs.2018.05.002
Received 25 September 2017; Received in revised form 7 April 2018; Accepted 8 May 2018
0924-2716/ © 2018 International Society for Photogrammetry and Remote Sensing, Inc. (ISPRS). Published by Elsevier B.V. All rights reserved.

Please cite this article as: Yang, R., ISPRS Journal of Photogrammetry and Remote Sensing (2018), https://doi.org/10.1016/j.isprsjprs.2018.05.002

observation and transformation parameter values. We then consider true and approximate errors for these parameters, and derive the registration model error analytically using the estimation value and transformation parameter variances. Finally, we derive the analytical model to evaluate target based point cloud registration error.

### 2.1. Registration model

Target based registration of two scans is the most common registration approach and is most often performed using 3D rigid body transformation algorithm (Zhang, 2008; Eggert et al., 1997; Yao et al., 2007). The registration model can be expressed as point clouds in ***Scan i+1*** are transformed into ***Scan i*** using the true values of three translation parameters $\widetilde{t_x}, \widetilde{t_y}, \widetilde{t_z}$ and three rotation parameters $\widetilde{a}, \widetilde{b}, \widetilde{c}$ (Zhang, 2008; Yang, 2011),

$$\widetilde{p}_j^i = \begin{bmatrix} \widetilde{x}_j^i \\ \widetilde{y}_j^i \\ \widetilde{z}_j^i \end{bmatrix} = \widetilde{R} \begin{bmatrix} \widetilde{x}_j^{i+1} \\ \widetilde{y}_j^{i+1} \\ \widetilde{z}_j^{i+1} \end{bmatrix} + \widetilde{T} = \widetilde{R}\widetilde{p}_j^{i+1} + \widetilde{T}, \tag{1}$$

where $\widetilde{p}_j^i$ and $\widetilde{p}_j^{i+1}$ represent the coordinate true values of the same point in ***Scan i*** and ***Scan i+1***, respectively, i.e., $(\widetilde{x}_j^i, \widetilde{y}_j^i, \widetilde{z}_j^i)$ and $(\widetilde{x}_j^{i+1}, \widetilde{y}_j^{i+1}, \widetilde{z}_j^{i+1})$;$\widetilde{T}$ is a $3 \times 1$ translation vector,

$$\widetilde{T} = \begin{bmatrix} \widetilde{t}_x \\ \widetilde{t}_y \\ \widetilde{t}_z \end{bmatrix}, \tag{2}$$

and $\widetilde{R}$ is a $3 \times 3$ rotation matrix,

$$\widetilde{R} = \frac{1}{1+\widetilde{a}^2+\widetilde{b}^2+\widetilde{c}^2} \begin{bmatrix} 1+\widetilde{a}^2-\widetilde{b}^2-\widetilde{c}^2 & 2(\widetilde{c}+\widetilde{a}\widetilde{b}) & 2(\widetilde{a}\widetilde{c}-\widetilde{b}) \\ 2(\widetilde{a}\widetilde{b}-\widetilde{c}) & 1-\widetilde{a}^2+\widetilde{b}^2-\widetilde{c}^2 & 2(\widetilde{a}+\widetilde{b}\widetilde{c}) \\ 2(\widetilde{b}+\widetilde{a}\widetilde{c}) & 2(\widetilde{b}\widetilde{c}-\widetilde{a}) & 1-\widetilde{a}^2-\widetilde{b}^2+\widetilde{c}^2 \end{bmatrix}, \tag{3}$$

$$\widetilde{R}^T = \widetilde{R}^{-1}, |\widetilde{R}| = 1. \tag{4}$$

Let $\widetilde{\eta} = [\widetilde{a}, \widetilde{b}, \widetilde{c}, \widetilde{t_x}, \widetilde{t_y}, \widetilde{t_z}]^T$ be the vector of transformation parameters. To uniquely determine $\widetilde{\eta}$ between ***Scan i*** and ***Scan i+1***, we normally use three or more targets with known 3D coordinates (Reshetyuk, 2009; Bornaz et al., 2003), placed in the overlaps between the two point clouds. This paper assumes the number of targets is $k$ ($\geqslant 3$), hence

$$\begin{bmatrix} \widetilde{p}_1^i \\ \widetilde{p}_2^i \\ \vdots \\ \widetilde{p}_k^i \end{bmatrix} = \begin{bmatrix} \widetilde{R}\widetilde{p}_1^{i+1} \\ \widetilde{R}\widetilde{p}_2^{i+1} \\ \vdots \\ \widetilde{R}\widetilde{p}_k^{i+1} \end{bmatrix} + \begin{bmatrix} \widetilde{T} \\ \widetilde{T} \\ \vdots \\ \widetilde{T} \end{bmatrix}. \tag{5}$$

### 2.2. Error equation of target based registration model

Errors inevitably occur in TLS measurements (including instrumental errors, environmental errors, object related errors, target centroid errors, saturation errors, blooming errors, etc. (Reshetyuk, 2009)). If the observation values of $\widetilde{p}_j^i$ and $\widetilde{p}_j^{i+1}$ are $p_j^i$ and $p_j^{i+1}$, respectively, and approximate values of $\widetilde{R}, \widetilde{T}, \widetilde{\eta}$ are $R_0, T_0, \eta_0$ ($\eta_0 = [a_0, b_0, c_0, t_{x0}, t_{y0}, t_{z0}]^T$ can be calculated by the method in Appendix C), then true errors of $p_j^i, p_j^{i+1}, R_0, T_0$, and $\eta_0$ are $\Delta_{p_j^i}, \Delta_{p_j^{i+1}}, \Delta_R, \Delta_T$, and $\Delta_\eta$ respectively, where

$$\widetilde{p}_j^i = p_j^i + \Delta_{p_j^i}, \widetilde{p}_j^{i+1} = p_j^{i+1} + \Delta_{p_j^{i+1}},$$

$$\widetilde{R} = R_0 + \Delta_{R_0}, \widetilde{T} = T_0 + \Delta_{T_0},$$

and

$$\widetilde{\eta} = \eta_0 + \Delta_{\eta_0}.$$

Hence, from Eq. (5),

$$v_j = \Delta_R \cdot p_j^{i+1} + \Delta_T - l_j, \tag{6}$$

where $l_j = p_j^i - R_0 p_j^{i+1} - T_0, j \in \{1, 2, ..., k\}$, $v_j = -(R_0 \Delta_{p_j^{i+1}} + \Delta_R \Delta_{p_j^{i+1}})$ is residual error.

Using the linearization theorem (Qiu et al., 2008),

$$\begin{cases} \Delta_R \approx dR = \frac{\partial R}{\partial a}da + \frac{\partial R}{\partial b}db + \frac{\partial R}{\partial c}dc \\ \Delta_T \approx dT = [dt_x, dt_y, dt_z]^T \\ \Delta_\eta \approx d\eta = [da, db, dc, dt_x, dt_y, dt_z]^T \end{cases}, \tag{7}$$

where $dR, dT, d\eta$ are the approximate values for $\Delta_R, \Delta_T, \Delta_\eta$, respectively.

We can construct the error equations of the target based registration model from Eqs. (6) and (7),

$$V \approx B \cdot d\eta - l, \tag{8}$$

where $V$ and $l$ are $3k \times 1$ matrices, $B$ is a $3k \times 6$ matrix,

$$V = \begin{bmatrix} v_1 \\ v_2 \\ \vdots \\ v_k \end{bmatrix}, B = \begin{bmatrix} B_1 \\ B_2 \\ \vdots \\ B_k \end{bmatrix}, l = \begin{bmatrix} l_1 \\ l_2 \\ \vdots \\ l_k \end{bmatrix}, v_j \approx dR \cdot p_j^{i+1} + dT - l_j = B_j \cdot d\eta - l_j, \tag{9}$$

$$R_0 = \frac{1}{1+a_0^2+b_0^2+c_0^2} \begin{bmatrix} 1+a_0^2-b_0^2-c_0^2 & 2(c_0+a_0b_0) & 2(a_0c_0-b_0) \\ 2(a_0b_0-c_0) & 1-a_0^2+b_0^2-c_0^2 & 2(a_0+b_0c_0) \\ 2(b_0+a_0c_0) & 2(b_0c_0-a_0) & 1-a_0^2-b_0^2+c_0^2 \end{bmatrix}, \tag{10}$$

$$T_0 = \begin{bmatrix} t_{x0} \\ t_{y0} \\ t_{z0} \end{bmatrix}, p_j^{i+1} = \begin{bmatrix} x_j^{i+1} \\ y_j^{i+1} \\ z_j^{i+1} \end{bmatrix}, \tag{11}$$

$$B_j = \begin{bmatrix} \frac{\partial R}{\partial a}p_j^{i+1} & \frac{\partial R}{\partial b}p_j^{i+1} & \frac{\partial R}{\partial c}p_j^{i+1} & E_{3\times3} \end{bmatrix}, E_{3\times3} = \begin{bmatrix} 1 & 0 & 0 \\ 0 & 1 & 0 \\ 0 & 0 & 1 \end{bmatrix}, \tag{12}$$

$$\begin{cases} \frac{\partial R}{\partial a} = \begin{bmatrix} \frac{4a_0(b_0^2+c_0^2)}{(1+a_0^2+b_0^2+c_0^2)^2} & \frac{2b_0(1-a_0^2+b_0^2+c_0^2)-4a_0c_0}{(1+a_0^2+b_0^2+c_0^2)^2} & \frac{2c_0(1-a_0^2+b_0^2+c_0^2)+4a_0b_0}{(1+a_0^2+b_0^2+c_0^2)^2} \\ \frac{2b_0(1-a_0^2+b_0^2+c_0^2)+4a_0c_0}{(1+a_0^2+b_0^2+c_0^2)^2} & \frac{-4a_0(1+b_0^2)}{(1+a_0^2+b_0^2+c_0^2)^2} & \frac{2(1-a_0^2+b_0^2+c_0^2)-4a_0b_0c_0}{(1+a_0^2+b_0^2+c_0^2)^2} \\ \frac{2c_0(1-a_0^2+b_0^2+c_0^2)-4a_0b_0}{(1+a_0^2+b_0^2+c_0^2)^2} & \frac{-2(1-a_0^2+b_0^2+c_0^2)-4a_0b_0c_0}{(1+a_0^2+b_0^2+c_0^2)^2} & \frac{-4a_0(1+c_0^2)}{(1+a_0^2+b_0^2+c_0^2)^2} \end{bmatrix} \\ \frac{\partial R}{\partial b} = \begin{bmatrix} \frac{-4b_0(1+a_0^2)}{(1+a_0^2+b_0^2+c_0^2)^2} & \frac{2a_0(1+a_0^2-b_0^2+c_0^2)-4b_0c_0}{(1+a_0^2+b_0^2+c_0^2)^2} & \frac{-2(1+a_0^2-b_0^2+c_0^2)-4a_0b_0c_0}{(1+a_0^2+b_0^2+c_0^2)^2} \\ \frac{2a_0(1+a_0^2-b_0^2+c_0^2)+4b_0c_0}{(1+a_0^2+b_0^2+c_0^2)^2} & \frac{4b_0(a_0^2+c_0^2)}{(1+a_0^2+b_0^2+c_0^2)^2} & \frac{2c_0(1+a_0^2-b_0^2+c_0^2)-4a_0b_0}{(1+a_0^2+b_0^2+c_0^2)^2} \\ \frac{2(1+a_0^2-b_0^2+c_0^2)-4a_0b_0c_0}{(1+a_0^2+b_0^2+c_0^2)^2} & \frac{2c_0(1+a_0^2-b_0^2+c_0^2)+4a_0b_0}{(1+a_0^2+b_0^2+c_0^2)^2} & \frac{-4b_0(1+c_0^2)}{(1+a_0^2+b_0^2+c_0^2)^2} \end{bmatrix} \\ \frac{\partial R}{\partial c} = \begin{bmatrix} \frac{-4c_0(1+a_0^2)}{(1+a_0^2+b_0^2+c_0^2)^2} & \frac{2(1+a_0^2+b_0^2-c_0^2)-4a_0b_0c_0}{(1+a_0^2+b_0^2+c_0^2)^2} & \frac{2a_0(1+a_0^2+b_0^2-c_0^2)+4b_0c_0}{(1+a_0^2+b_0^2+c_0^2)^2} \\ \frac{-2(1+a_0^2+b_0^2-c_0^2)-4a_0b_0c_0}{(1+a_0^2+b_0^2+c_0^2)^2} & \frac{-4c_0(1+b_0^2)}{(1+a_0^2+b_0^2+c_0^2)^2} & \frac{2b_0(1+a_0^2+b_0^2-c_0^2)-4a_0c_0}{(1+a_0^2+b_0^2+c_0^2)^2} \\ \frac{2a_0(1+a_0^2+b_0^2-c_0^2)-4b_0c_0}{(1+a_0^2+b_0^2+c_0^2)^2} & \frac{2b_0(1+a_0^2+b_0^2-c_0^2)+4a_0c_0}{(1+a_0^2+b_0^2+c_0^2)^2} & \frac{4c_0(a_0^2+b_0^2)}{(1+a_0^2+b_0^2+c_0^2)^2} \end{bmatrix} \end{cases}. \tag{13}$$

Assuming the weight matrix of $l$ is $P$, by using the principle of indirect adjustment (Qiu et al., 2008) and $V^TPV = min$, we can obtain estimated $\hat{\eta}, \hat{R}, \hat{T}$ for transformation parameters $\widetilde{\eta}, \widetilde{R}, \widetilde{T}$ as

$$\widetilde{\eta} \approx \hat{\eta} = [\hat{a} \quad \hat{b} \quad \hat{c} \quad \hat{t_x} \quad \hat{t_y} \quad \hat{t_z}]^T = \eta_0 + d\eta, \tag{14}$$

$$d\eta = (B^T PB)^{-1} B^T Pl, \tag{15}$$

and

$$\widetilde{R} \approx \hat{R} = \frac{1}{1+\hat{a}^2+\hat{b}^2+\hat{c}^2} \begin{bmatrix} 1+\hat{a}^2-\hat{b}^2-\hat{c}^2 & 2(\hat{a}\hat{b}+\hat{c}) & 2(\hat{a}\hat{c}-\hat{b}) \\ 2(\hat{a}\hat{b}-\hat{c}) & 1-\hat{a}^2+\hat{b}^2-\hat{c}^2 & 2(\hat{b}\hat{c}+\hat{a}) \\ 2(\hat{a}\hat{c}+\hat{b}) & 2(\hat{b}\hat{c}-\hat{a}) & 1-\hat{a}^2-\hat{b}^2+\hat{c}^2 \end{bmatrix}, \tag{16}$$

$$\widetilde{T} \approx \hat{T} = \begin{bmatrix} \hat{t_x} \\ \hat{t_y} \\ \hat{t_z} \end{bmatrix}. \tag{17}$$

If $\sigma_0$ is the unit weight variance (usually determined in initial processing before registration), then from error propagation (Qiu et al., 2008) and Eq. (15), the variance and covariance of $\hat{\eta}$ can be expressed as

$$D_{\hat{\eta}\hat{\eta}} = \sigma_0^2 Q_{\hat{\eta}\hat{\eta}} = \sigma_0^2 Q_{d\eta d\eta} = \sigma_0^2 N_{BB}^{-1} = \sigma_0^2 (B^T PB)^{-1}, \tag{18}$$

where $D_{\hat{\eta}\hat{\eta}}$ is a $6 \times 6$ matrix.

### 2.3. Target based point cloud registration error evaluation

We can obtain the actual registration value $\hat{p}^i$ for any point $p^{i+1}$ from Eqs. (16) and (17),

$$\hat{p}^i = \hat{R} p^{i+1} + \hat{T}, \tag{19}$$

where the registration error of $\hat{p}^i$ is influenced by both $\hat{\eta}$ and $p^{i+1}$ precision.

Therefore, partial differentiation of Eq. (19) shows that

$$d\hat{p}^i = d\hat{R} \cdot p^{i+1} + d\hat{T} + \hat{R} \cdot dp^{i+1}, \tag{20}$$

where

$$p^{i+1} = \begin{bmatrix} x^{i+1} \\ y^{i+1} \\ z^{i+1} \end{bmatrix}, \quad B_{p^{i+1}} = \begin{bmatrix} \frac{\partial \hat{R}}{\partial a} p^{i+1} & \frac{\partial \hat{R}}{\partial b} p^{i+1} & \frac{\partial \hat{R}}{\partial c} p^{i+1} & E_{3\times 3} \end{bmatrix}, \tag{21}$$

and

$$\begin{cases} \frac{\partial \hat{R}}{\partial a} = \begin{bmatrix} \frac{4\hat{a}(\hat{b}^2+\hat{c}^2)}{(1+\hat{a}^2+\hat{b}^2+\hat{c}^2)^2} & \frac{2\hat{b}(1-\hat{a}^2+\hat{b}^2+\hat{c}^2)-4\hat{a}\hat{c}}{(1+\hat{a}^2+\hat{b}^2+\hat{c}^2)^2} & \frac{2\hat{c}(1-\hat{a}^2+\hat{b}^2+\hat{c}^2)+4\hat{a}\hat{b}}{(1+\hat{a}^2+\hat{b}^2+\hat{c}^2)^2} \\ \frac{2\hat{b}(1-\hat{a}^2+\hat{b}^2+\hat{c}^2)+4\hat{a}\hat{c}}{(1+\hat{a}^2+\hat{b}^2+\hat{c}^2)^2} & \frac{-4\hat{a}(1+\hat{b}^2)}{(1+\hat{a}^2+\hat{b}^2+\hat{c}^2)^2} & \frac{2(1-\hat{a}^2+\hat{b}^2+\hat{c}^2)-4\hat{a}\hat{b}\hat{c}}{(1+\hat{a}^2+\hat{b}^2+\hat{c}^2)^2} \\ \frac{2\hat{c}(1-\hat{a}^2+\hat{b}^2+\hat{c}^2)-4\hat{a}\hat{b}}{(1+\hat{a}^2+\hat{b}^2+\hat{c}^2)^2} & \frac{-2(1-\hat{a}^2+\hat{b}^2+\hat{c}^2)-4\hat{a}\hat{b}\hat{c}}{(1+\hat{a}^2+\hat{b}^2+\hat{c}^2)^2} & \frac{-4\hat{a}(1+\hat{c}^2)}{(1+\hat{a}^2+\hat{b}^2+\hat{c}^2)^2} \end{bmatrix} \\ \frac{\partial \hat{R}}{\partial b} = \begin{bmatrix} \frac{-4\hat{b}(1+\hat{a}^2)}{(1+\hat{a}^2+\hat{b}^2+\hat{c}^2)^2} & \frac{2\hat{a}(1+\hat{a}^2-\hat{b}^2+\hat{c}^2)-4\hat{b}\hat{c}}{(1+\hat{a}^2+\hat{b}^2+\hat{c}^2)^2} & \frac{-2(1+\hat{a}^2-\hat{b}^2+\hat{c}^2)-4\hat{a}\hat{b}\hat{c}}{(1+\hat{a}^2+\hat{b}^2+\hat{c}^2)^2} \\ \frac{2\hat{a}(1+\hat{a}^2-\hat{b}^2+c\hat{c}^2)+4\hat{b}\hat{c}}{(1+\hat{a}^2+\hat{b}^2+\hat{c}^2)^2} & \frac{4\hat{b}(\hat{a}^2+\hat{c}^2)}{(1+\hat{a}^2+\hat{b}^2+\hat{c}^2)^2} & \frac{2\hat{c}(1+\hat{a}^2-\hat{b}^2+\hat{c}^2)-4\hat{a}\hat{b}}{(1+\hat{a}^2+\hat{b}^2+\hat{c}^2)^2} \\ \frac{2(1+\hat{a}^2-\hat{b}^2+\hat{c}^2)-4\hat{a}\hat{b}\hat{c}}{(1+\hat{a}^2+\hat{b}^2+\hat{c}^2)^2} & \frac{2\hat{c}(1+\hat{a}^2-\hat{b}^2+\hat{c}^2)+4\hat{a}\hat{b}}{(1+\hat{a}^2+\hat{b}^2+\hat{c}^2)^2} & \frac{-4\hat{b}(1+\hat{c}^2)}{(1+\hat{a}^2+\hat{b}^2+\hat{c}^2)^2} \end{bmatrix} \\ \frac{\partial \hat{R}}{\partial c} = \begin{bmatrix} \frac{-4\hat{c}(1+\hat{a}^2)}{(1+\hat{a}^2+\hat{b}^2+\hat{c}^2)^2} & \frac{2(1+\hat{a}^2+\hat{b}^2-\hat{c}^2)-4\hat{a}\hat{b}\hat{c}}{(1+\hat{a}^2+\hat{b}^2+\hat{c}^2)^2} & \frac{2\hat{a}(1+\hat{a}^2+\hat{b}^2-\hat{c}^2)+4\hat{b}\hat{c}}{(1+\hat{a}^2+\hat{b}^2+\hat{c}^2)^2} \\ \frac{-2(1+\hat{a}^2+\hat{b}^2-\hat{c}^2)-4\hat{a}\hat{b}\hat{c}}{(1+\hat{a}^2+\hat{b}^2+\hat{c}^2)^2} & \frac{-4\hat{c}(1+\hat{b}^2)}{(1+\hat{a}^2+\hat{b}^2+\hat{c}^2)^2} & \frac{2\hat{b}(1+\hat{a}^2+\hat{b}^2-\hat{c}^2)-4\hat{a}\hat{c}}{(1+\hat{a}^2+\hat{b}^2+\hat{c}^2)^2} \\ \frac{2\hat{a}(1+\hat{a}^2+\hat{b}^2-\hat{c}^2)-4\hat{b}\hat{c}}{(1+\hat{a}^2+\hat{b}^2+\hat{c}^2)^2} & \frac{2\hat{b}(1+\hat{a}^2+\hat{b}^2-\hat{c}^2)+4\hat{a}\hat{c}}{(1+\hat{a}^2+\hat{b}^2+\hat{c}^2)^2} & \frac{4\hat{c}(\hat{a}^2+\hat{b}^2)}{(1+\hat{a}^2+\hat{b}^2+\hat{c}^2)^2} \end{bmatrix} \end{cases}. \tag{22}$$

Assuming coordinate measurements for any point $p^{i+1}$ have independent and identical distributions, and the variance of coordinate error of $p^{i+1}$ is $D_{p_{i+1}p_{i+1}} = \sigma^2_{p^{i+1}} E_{3\times 3}$, then from Eq. (20),

$$D_{\hat{p}^i\hat{p}^i} = D_{PRE}(p^{i+1}) + D_{ORE}(p^{i+1}), \tag{23}$$

$$D_{PRE}(p^{i+1}) = B_{p^{i+1}} D_{\hat{\eta}\hat{\eta}} B^T_{p^{i+1}}, \tag{24}$$

and

$$D_{ORE}(p^{i+1}) = \hat{R} D_{p^{i+1}p^{i+1}} \hat{R}^T = D_{p^{i+1}p^{i+1}}, \tag{25}$$

where $D_{\hat{p}^i\hat{p}^i}$ is the registration error (***RE***) of $p^{i+1}$, $D_{PRE}(p^{i+1})$ is the propagated registration error (***PRE***) of $p^{i+1}$, and $D_{ORE}(p^{i+1})$ is the observation registration error (***ORE***) of $p^{i+1}$.

From Eqs. (23)–(25), ***RE*** for any point $p^{i+1}$ is related to its coordinate value in ***Scan i+1*** (influencing $B_{p^{i+1}}$), transformation parameter precision (influencing $D_{\hat{\eta}\hat{\eta}}$), and observation precision (influencing $D_{p^{i+1}p^{i+1}}$). ***ORE*** for $p^{i+1}$ is unchanged by the transformation.

## 3. Verification

We first introduce the experiment method (including constraint conditions), analyze ***RE*** model influencing factors, and propose a method to verifying ***RE*** model accuracy. We then design the experiment to verify that rotation parameters do not influence ***PRE***. Finally, based on these outcomes, we design the experiment to verifying the proposed ***RE*** model accuracy, and analyze the experimental results.

### 3.1. Experiment method

To verify ***RE*** model accuracy (Eq. (23)), we design several processing schemes with realistic point clouds drawn from previous studies (Yang, 2011) using Riegl VZ-400 laser scanner, as shown in Figs. 1 and 2. The specific experimental processes are as follows:

***Step1:*** Point cloud extraction.
We included three practical point cloud types. ***case A***: completely within (Fig. 2, red zone), ***case B***: partially within and partially outside (Fig. 2, pink zone), and ***case C***: completely outside (Fig. 2, yellow zone) the targets convex polyhedron. We extracted these three point cloud types from realistic point clouds.
***Step2:*** Constraint conditions.
Similar to (Fan et al., 2015), we make the following assumptions:
(1) Unit weight variance $\sigma_0 = 5$ mm, since Riegl VZ-400 laser scanner acquisition error = 5 mm@50 m (Yang, 2011).
(2) Target coordinate measurement error for ***Scan i+1*** is isotropic, targets are independent and have equal standard deviation. Hence $P$, target measurement weight matrix, is diagonal matrix with equal diagonal elements.
***Step3:*** Rotation parameter influences.
Since ***ORE*** is unchanged after transformation (Eq. (25)), ***RE*** only depends on ***PRE*** magnitude (Eq. (24)), ***PRE*** is related to $B_{p^{i+1}}$ and $D_{\hat{\eta}\hat{\eta}}$, and $B_{p^{i+1}}$ is only related to $p^{i+1}$ coordinates and $\hat{a}$, $\hat{b}$ and $\hat{c}$ (Eqs. (21) and (22)). Therefore, we need only investigate whether different rotation parameter values influence ***PRE*** (Eq. (24)).
Appendix A shows that the rotation parameters can be calculated from the rotation angle and axis, hence we can analyze ***PRE*** variation by fixing each of these independently.
***Step4:*** Verify ***RE*** model accuracy.
We adopt the root mean square error (***RMSE***) to evaluate true errors magnitude (Fan et al., 2015). For any point $p^{i+1}$ in ***Scan i+1***, we can calculate true registration errors, ***RMSE***, from Eqs. (1) and (19) as

$$\boldsymbol{RMSE} = \sqrt{\frac{1}{m}\sum_{s=1}^{m} \Delta_s^2}, \tag{26}$$

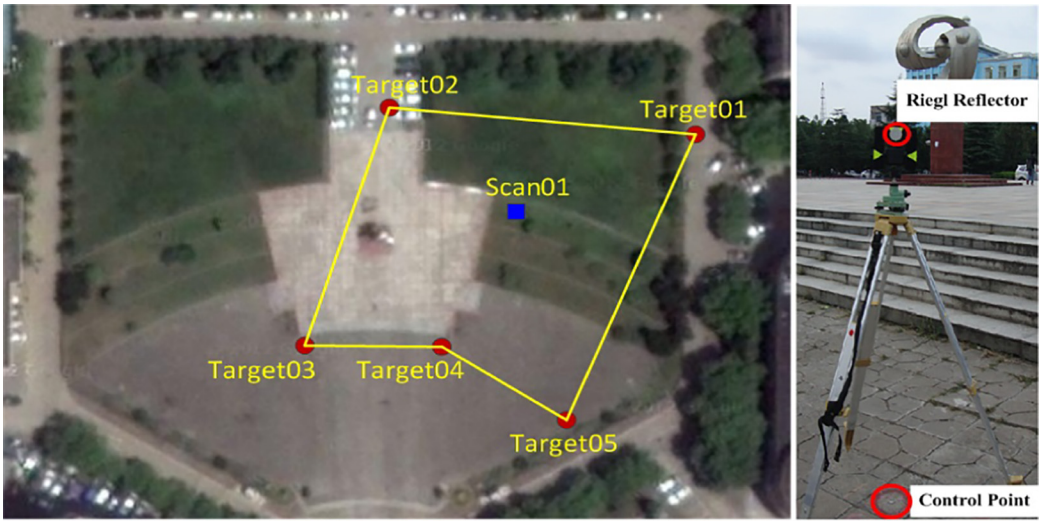


**Fig. 1.** Experimental target geometry.

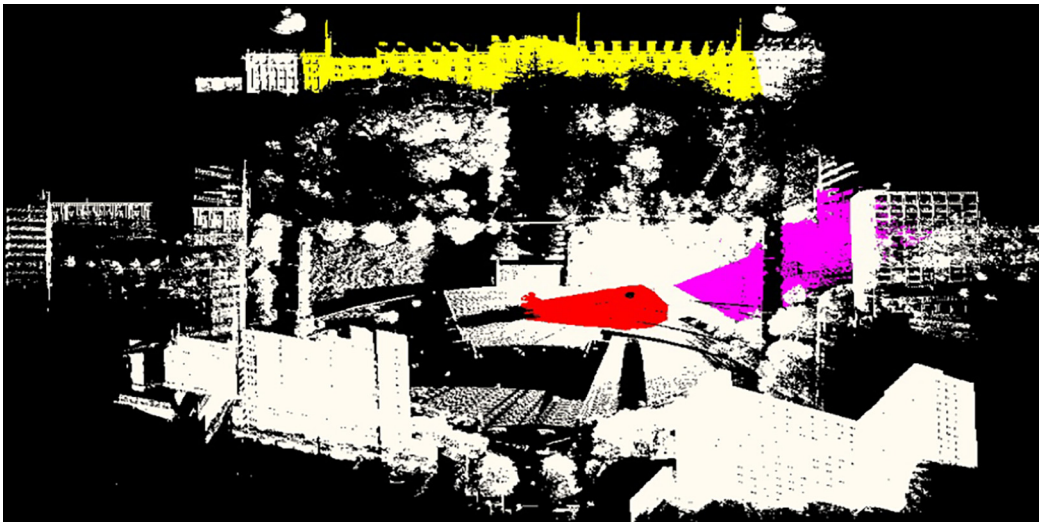

**Fig. 2.** Measured point cloud. (***case A*** = red, ***case B*** = pink, and ***case C*** = yellow). (For interpretation of the references to color in this figure legend, the reader is referred to the web version of this article.)

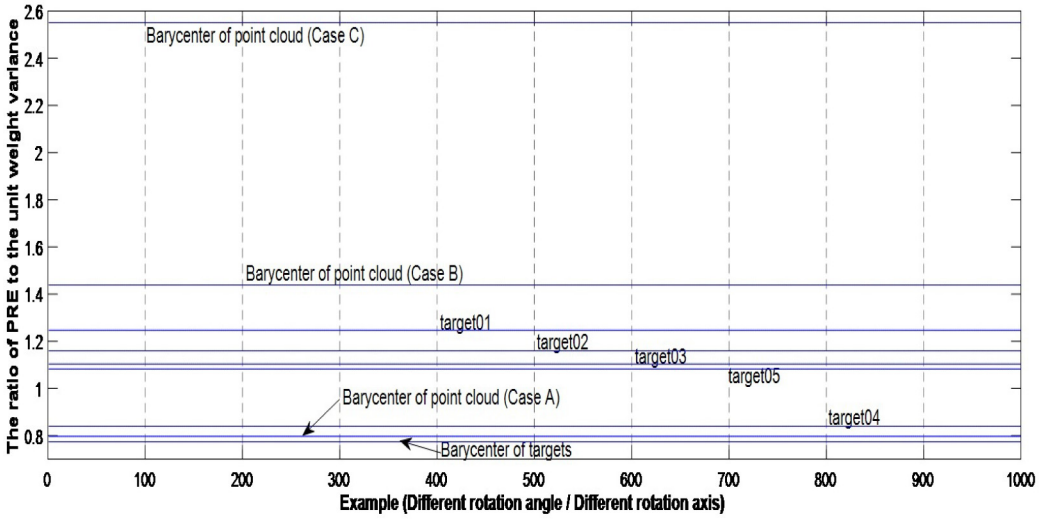


**Fig. 3.** Rotation parameter influence. (Each x axis value represents a different rotation matrix case, i.e. different rotatin angle and axis; Each y axis represents a ratio of ***PRE*** to $\sigma_0$.)

**Table 1**
The relationship between the position and ***PRE***.

| Position | | Distance (to Barycenter of targets) | Ratio (**PRE** to $\sigma_0$) |
|---|---|---|---|
| target01 | | 45.393 m | 1.248 |
| target02 | | 36.263 m | 1.161 |
| target03 | | 32.980 m | 1.104 |
| target04 | | 14.745 m | 0.840 |
| target05 | | 34.768 m | 1.083 |
| point cloud barycenter | ***case A*** | 8.151 m | 0.797 |
| | ***case B*** | 56.018 m | 1.439 |
| | ***case C*** | 104.285 | 2.552 |
| targets barycenter | | 0 | 0.775 |

where

$$\Delta_s = (\widetilde{R}-\widehat{R})p_s^{i+1} + (\widetilde{T}-\widehat{T}), \tag{27}$$

and $p_s^{i+1}$ is the s-th sampling value of point $p^{i+1}$;$s = 1, \ldots, m$;$m$ is the total number of random samples.

Thus, we compare ***RE*** from Eqs. (23)–(25) with ***RMSE*** from Eqs. (26) and (27).

### 3.2. Rotation parameter influences

We randomly generate 1000 rotation axes for a fixed rotation angle (Eqs. (A.1) and (A.2)) and calculate $D_{\hat{\eta}\hat{\eta}}$ from Eqs. (12), (13), and (18) using target observations. We then calculate target ***PRE***, targets

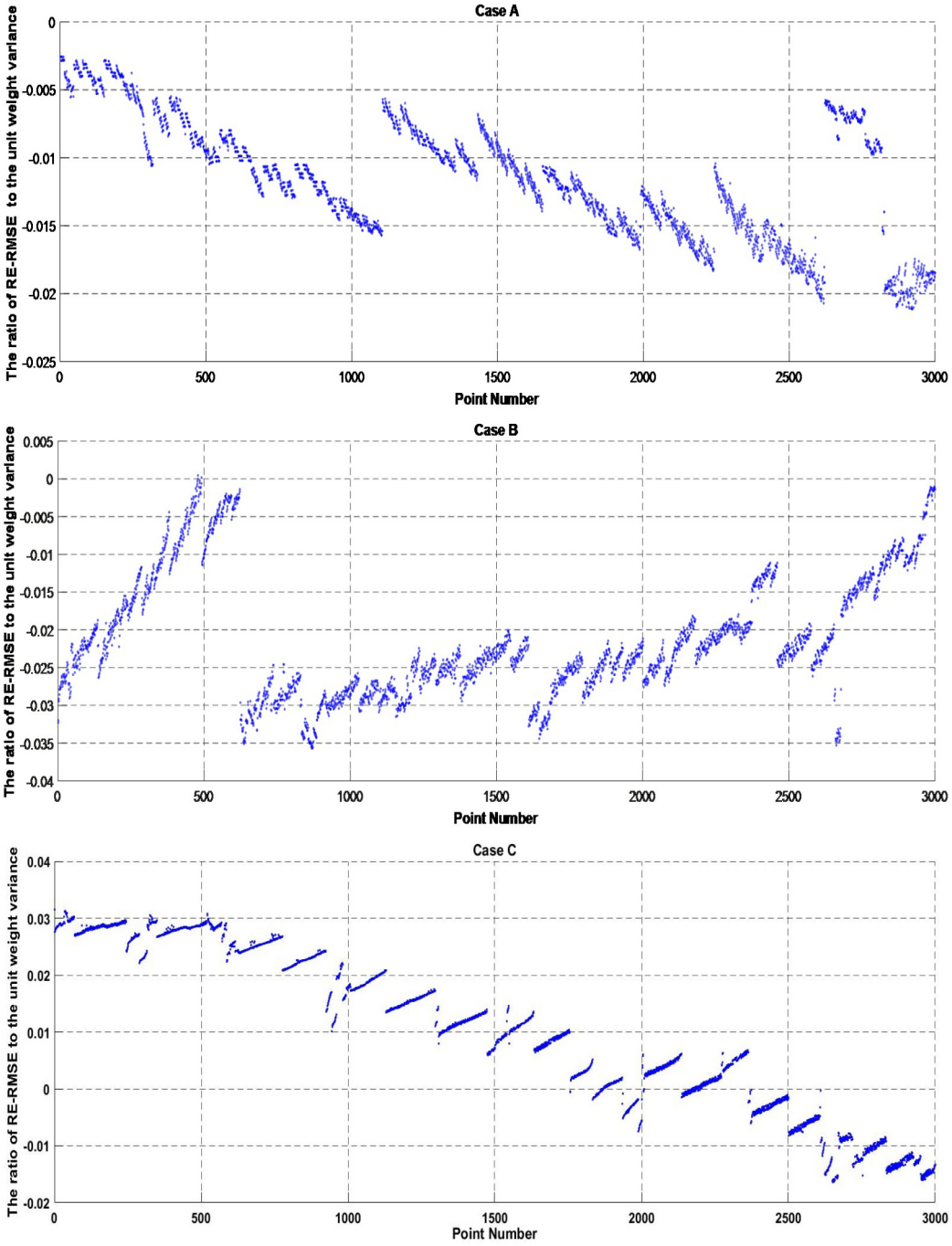


**Fig. 4.** The difference between ***RE*** and ***RMSE***. (Each x axis value represents a different point in the point cloud of ***case A, B, C***; Each y axis represents a ratio of ***RE-RMSE*** to $\sigma_0$.)

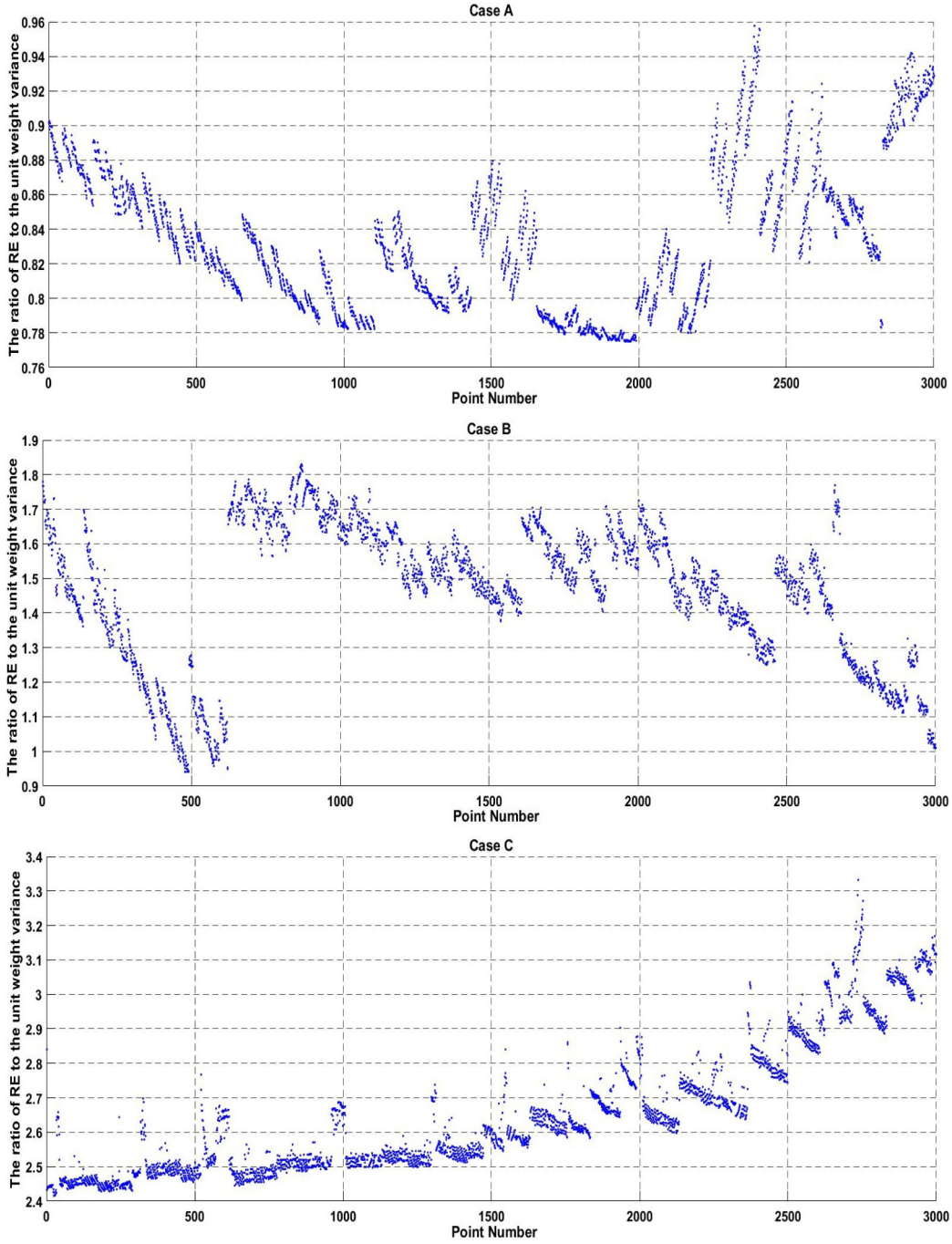


**Fig. 5.** Point cloud registration error from the proposed method (***RE***) for ***case A, B, C*** point cloud. (Each x axis value represents a different point; Each y axis represents a ratio of ***RE*** to $\sigma_0$.)

barycenter ***PRE***, and point cloud barycenter ***PRE*** for ***case A***, ***case B***, ***case C*** using Eqs. (21), (22), and (24), respectively. Similarly, we randomly generate 1000 rotation angles for a fixed rotation axis, and calculate $D_{\hat{\eta}\hat{\eta}}$, target ***PRE***, targets barycenter ***PRE***, and point cloud barycenter ***PRE***.

Fig. 3 and Table 1 show that rotation parameters have no ***PRE*** influence for any point, and ***PRE*** is inversely proportional to distance to the targets barycenter. Thus, target registration errors are not equal to point cloud registration errors.

### 3.3. *RE model accuracy*

We calculate $D_{\hat{\eta}\hat{\eta}}$ from Eqs. (12), (13), and (18) using target observations, and randomly generate 1000 different approximate errors, $d\eta$, for the transformation parameters using $D_{\hat{\eta}\hat{\eta}}$. Since ***RE*** is independent of the rotation parameters (Section 3.2), we can assume

$$\tilde{\eta} = \eta_0 = [0 \quad 0 \quad 0 \quad 100 \quad 100 \quad 100]^T. \tag{28}$$

We then calculate 1000 different $\hat{\eta}$, and the ***RMSE*** for all points in ***case A, B, C*** point clouds from Eqs. (26), (27), (2) and (3), (16), and (17).

Finally, we set $\hat{\eta} = \eta_0$, and calculate ***RE*** for all points in ***case A, B, C*** point clouds from Eqs. (21)–(25).

Figs. 4 and 5 compare the ***RE*** and ***RMSE*** outcomes for the various cases. Maximum ***RE*** and ***RMSE*** differences are less than $-0.022\sigma_0$, $-0.035\sigma_0$, and $0.03\sigma_0$ for in ***case A, B, C***, respectively. These

differences are sufficiently small that we can consider ***RE*** ≡ ***RMSE***, i.e., the proposed ***RE*** model is correct.

Commercial software can only calculate target registration errors of targets, and for these experimental data, target registration error calculated by Leica cyclone are $1.163\sigma_0$, $1.070\sigma_0$, $0.998\sigma_0$, $0.746\sigma_0$, and $0.962\sigma_0$, for targets 01, 02, 03, 04, and 05, respectively. Each point in the point cloud has different accuracy, which cannot be evaluated by several numerical values (such as target registration errors). Hence, the proposed ***RE*** model is superior to current commercial software to evaluate point cloud registration error.

## 4. Conclusion

This paper investigate point cloud registration error (***RE***) magnitude analytically, and derive a new competent evaluation model of point cloud ***RE*** model. We verify the registration error from the proposed ***RE*** model and the true error statistics ***RMSE*** are significantly smaller ($< 0.035\sigma_0$). Thus, the proposed ***RE*** model can directly evaluate point cloud registration error. Several relevant conclusions are evident: (1) Registration error (***RE***) for any point in space included propagated registration error (***PRE***) and observation registration error (***ORE***); (2) ***ORE*** for any point in a point cloud is only related to its observation precision, and is unchanged after registration, provided coordinate measurements for any point have independent and identical distribution; (3) ***PRE*** for any point in a point cloud is related to its position and registration parameter precisions, but is independent of rotation parameters; (4) ***PRE*** is related to the distance from the targets barycenter, i.e., increased ***PRE*** with increasing distance, thus the commercial evaluation models of point cloud registration error are only suitable to evaluate target registration errors, and are unsuitable to evaluate point cloud registration errors.

However, it should be noted that "before we use the proposed model, the coordinates information of targets need to be extracted using feature extraction algorithms", "our model is only suitable to evaluate the feature based registration error, including sphere target, plane target, natural features, building corner, etc.", "the relationship between the ***PRE*** and the rotation-parameter requires further analytical investigation" and "we do not consider the effects of linearization errors or coefficient matrix errors".

## Acknowledgment

This work is supported by the National Natural Science Foundation of China (grant 41304001), Chongqing Natural Science Foundation and Frontier Research Planning Project (grant cstc2014jcyjA00011), Chongqing Postdoctoral Research Project (grant xm2017097), Chongqing Natural Science Foundation and Technology Innovation Special Project of Social Undertaking and Peoples Livelihood Guarantee (grant cstc2016shmszx0299).

## Appendix A. Rotation parameters from rotation axis and angle

Following (Yang, 2011; Yao et al., 2007), if the rotation angle is $\theta$ and rotation axis is $\vec{n}$, then we can express the quaternions, $q$, of rotation-matrix $\widetilde{R}$ as

$$q = \begin{bmatrix} \cos\frac{\theta}{2} \\ \sin\frac{\theta}{2}\cdot\vec{n} \end{bmatrix}, \tag{A.1}$$

and hence the rotation parameters are

$$\begin{bmatrix} \widetilde{a} \\ \widetilde{b} \\ \widetilde{c} \end{bmatrix} = \tan\frac{\theta}{2}\cdot\vec{n}. \tag{A.2}$$

## Appendix B. Lodrigues matrix

The Lodrigues Matrix (Yao et al., 2007) is a rotation matrix composed of real skew symmetric matrix, and we can express the Lodrigues Matrix of the rotation-matrix $\widetilde{R}$ as

$$\widetilde{R} = (E_{3\times3} + \widetilde{S})^{-1}(E_{3\times3} - \widetilde{S}) = (E_{3\times3} - \widetilde{S})(E_{3\times3} + \widetilde{S})^{-1}, \tag{B.1}$$

where $\widetilde{S}$ is a real skew symmetric matrix, and

$$\widetilde{S} = \begin{bmatrix} 0 & -\widetilde{c} & \widetilde{b} \\ \widetilde{c} & 0 & -\widetilde{a} \\ -\widetilde{b} & \widetilde{a} & 0 \end{bmatrix}. \tag{B.2}$$

Thus, from Eqs. (3) and (B.2), we can get

$$(E_{3\times3} + \widetilde{S})\widetilde{R} = E_{3\times3} - \widetilde{S}. \tag{B.3}$$

Assuming $\widetilde{T} = 0$, from Eqs. (1) and (B.3), we can get

$$(E_{3\times3} + \widetilde{S})\begin{bmatrix} \widetilde{x}^i \\ \widetilde{y}^i \\ \widetilde{z}^i \end{bmatrix} = (E_{3\times3} - \widetilde{S})\begin{bmatrix} \widetilde{x}^{i+1} \\ \widetilde{y}^{i+1} \\ \widetilde{z}^{i+1} \end{bmatrix}, \tag{B.4}$$

and hence,

$$\begin{bmatrix} 0 & -(\widetilde{z}^i + \widetilde{z}^{i+1}) & \widetilde{y}^i + \widetilde{y}^{i+1} \\ \widetilde{z}^i + \widetilde{z}^{i+1} & 0 & -(\widetilde{x}^i + \widetilde{x}^{i+1}) \\ -(\widetilde{y}^i + \widetilde{y}^{i+1}) & \widetilde{x}^i + \widetilde{x}^{i+1} & 0 \end{bmatrix}\begin{bmatrix} \widetilde{a} \\ \widetilde{b} \\ \widetilde{c} \end{bmatrix} = \begin{bmatrix} \widetilde{x}_{i+1} - \widetilde{x}_i \\ \widetilde{y}_{i+1} - \widetilde{y}_i \\ \widetilde{z}_{i+1} - \widetilde{z}_i \end{bmatrix}. \tag{B.5}$$

## Appendix C. Approximate target transformation parameters

We can compute the approximation $\eta_0 = [a_0, b_0, c_0, t_{x0}, t_{y0}, t_{z0}]^T$ of $\tilde{\eta}$ from Eq. (B.5) (Yao et al., 2007) using the following steps.

***Step1:*** Compute targets barycenter coordinates,

$$p_c^i = \begin{bmatrix} \frac{\sum_{j=1}^k x_j^i}{k} \\ \frac{\sum_{j=1}^k y_j^i}{k} \\ \frac{\sum_{j=1}^k z_j^i}{k} \end{bmatrix}, p_c^{i+1} = \begin{bmatrix} \frac{\sum_{j=1}^k x_j^{i+1}}{k} \\ \frac{\sum_{j=1}^k y_j^{i+1}}{k} \\ \frac{\sum_{j=1}^k z_j^{i+1}}{k} \end{bmatrix}. \tag{C.1}$$

***Step2:*** Centralize the target coordinates,

$$p_{jc}^i = p_j^i - p_c^i, p_c^{i+1} = p_j^{i+1} - p_c^{i+1}. \tag{C.2}$$

***Step3:*** Calculate the coefficient matrices from the centralized target coordinates,

$$A_c = \begin{bmatrix} A_{1c} \\ \vdots \\ A_{kc} \end{bmatrix}, \tag{C.3}$$

$$l_c = \begin{bmatrix} l_{1c} \\ \vdots \\ l_{kc} \end{bmatrix}, \tag{C.4}$$

where $A_c$ is a $3k \times 3$ matrix, $l_c$ is a $3k \times 1$ matrix, $j = 1, \ldots, k$, and

$$A_{jc} = \begin{bmatrix} 0 & -(z_{jc}^i + z_{jc}^{i+1}) & y_{jc}^i + y_{jc}^{i+1} \\ z_{jc}^i + z_{jc}^{i+1} & 0 & -(x_{jc}^i + x_{jc}^{i+1}) \\ -(y_{jc}^i + y_{jc}^{i+1}) & x_{jc}^i + x_{jc}^{i+1} & 0 \end{bmatrix}, \tag{C.5}$$

$$l_{jc} = \begin{bmatrix} x_{jc}^{i+1} - x_{jc}^i \\ y_{jc}^{i+1} - y_{jc}^i \\ z_{jc}^{i+1} - z_{jc}^i \end{bmatrix}, \tag{C.6}$$

***Step4:*** Compute approximate rotation parameters

$$\begin{bmatrix} a_0 \\ b_0 \\ c_0 \end{bmatrix} = (A_c^T P A_c)^{-1} A_c^T P l_c, \tag{C.7}$$

where $P$ is the target weight matrix.

***Step5:*** Compute the approximate rotation matrix, $R_0$, from Eq. (10).

***Step6:*** Compute the approximate translation parameters

$$\begin{bmatrix} t_{x0} \\ t_{y0} \\ t_{z0} \end{bmatrix} = p_c^{i+1} - R_0 p_c^i. \tag{C.8}$$

## References

Arun, K.S., Huang, T.S., Blostein, S.D., 1987. Least-squares fitting of two 3D point sets. IEEE Trans. Pattern Anal. Mach. Intell. 9 (5), 698–700.

Besl, P.J., Mckay, H.D., 1992. A method for registration of 3-D shapes. IEEE Trans. Pattern Anal. Mach. Intell. 14 (2), 239–256.

Bornaz, L., Lingus, A., Rinaudo, F., 2003. Multiple scan registration in LiDAR close- range applications. In: Proceedings of the International Archives of the Photogrammetry: Remote Sensing and Spatial Information Sciences, 2003, Part 5/W12, vol. XXXIV, pp. 72–77.

Carmichael, O., Huber, D.F., Hebert, M., 1999. Large data sets and confusing scenes in 3-D surface matching and recognition. In: Proceedings of 2nd International Conference on 3D Digital Imaging and Modeling, 1999, pp. 358–367.

Chow, C.K., Tsui, H.T., Lee, T., 2004. Surface registration using a dynamic genetic algorithm. Pattern Recogn. 37 (1), 105–117.

Chuang, D.H., Yun, I.D., Lee, S.U., 1998. Registration of multiple-range views using the reverse-calibration technique. Pattern Recogn. 31 (4), 457–464.

Eggert, D.W., Lorusso, A., Fisher, R.B., 1997. Estimating 3-D rigid body transformations: a comparison of four major algorithms. Mach. Vision Appl. 9 (5–6), 272–290.

Fan, L., Smethurst, J.A., Atkinson, P.M., Powrie, W., 2015. Error in target-based georeferencing and registration in terrestrial laser scanning. Comput. Geosci. 83, 54–64.

Faugeras, O.D., Hebert, M., 1986. The representation, recognition, and locating of 3-D objects. Int. J. Robot. Res. 5 (3), 27–52.

Gordon, S.J., Lichti, D.D., 2004. Terrestrial laser scanners with a narrow field of view: the effect on 3D resection solutions. Surv. Rev. 37 (292), 448–468.

Harvey, B.R., 2004. Registration and transformation of multiple site terrestrial laser scanning. Geomatics Res. Austral. (80), 33–50.

Horn, B.K.P., 1987. Closed-form solution of absolute orientation using unit quaternions. J. Opt. Soc. Am. A 4 (4), 629–642.

Horn, B.K.P., Hilden, H.M., Negahdaripour, S., 1988. Closed-form solution of absolute orientation using orthonormal matrices. J. Opt. Soc. Am. A 5 (7), 1127–1135.

Lichti, D., Skaloud, J., 2010. Registration and calibration. In: Vosselman, G., Maas, H.G. (Eds.). Airborne and Terrestrial Laser Scanning. Whittles Publishing. ISBN: 190444587X. (Chapter 3).

Lichti, D.D., Gordon, S.J., Tipdecho, T., 2005. Error models and propagation in directly georeferenced terrestrial laser scanner networks. J. Surv. Eng. 131 (4), 135–142.

Qiu, W.N., Tao, B.Z., Yao, Y.B., Wu, Y., Huang, H.L., 2008. The Theory and Method of Surveying Data Processing, first ed. Wuhan University press, Wuhan China, pp. 1–6.

Reshetyuk, Y., 2009. Self-calibration and Direct Georeferencing in Terrestrial Laser Scanning (Ph.D. dissertation). Royal Institute of Technology, Swedish.

Salvi, J., Matabosch, C., Fofi, D., Forest, J., 2007. A review of recent range image registration methods with accuracy evaluation. Image Vision Comput. 25 (5), 578–596.

Sharp, G.C., Lee, S.W., Wehe, D.K., 2004. Multiview registration of 3D scenes by minimizing error between coordinate frames. IEEE Trans. Pattern Anal. Mach. Intell. 26 (8), 1037–1050.

Stamos, I., Leordeanu, M., 2003. Automated feature-based range registration of urban scenes of large scale. In: Proceedings of IEEE Computer Society Conference on Computer Vision and Pattern Recognition, 2003, pp. 555–561.

Tarel, J.P., Civi, H., Cooper, D.B., 1998. Pose estimation of free-form 3D objects without point matching using algebraic surface models. In: Proceedings of IEEE Workshop on Model-based 3D, pp. 13–21.

Walker, M.W., Shao, L.J., 1991. Estimating 3-D location parameters using dual number quaternions. CVGIP: Image Understand. 54 (3), 358–367.

Wang, G.L., 2006. Research on Registration of Ground Lidar Range Images (Masters dissertation). Beijing University of Civil Engineering and Architecture, Beijing China.

Yang, R.H., 2011. Research on Point Cloud Angular Resolution and Processing Model of Terrestrial Laser Scanning (Ph.D. dissertation). Wuhan University, Wuhan China.

Yao, Jili, Xu, Yufei, Xiao, Wei, 2007. Application of Lodrigues Matrix in 3D coordinate transformation. Geomatics Informat. Sci. Wuhan Univ. 10 (3), 173–176.

Zhang, Y., 2008. Research on Point Cloud Processing of Terrestrial Laser Scanning (Ph.D. dissertation). Wuhan University, Wuhan China.

Zhang, Y., 2012. Research on error propagation of point cloud registration. In: Proceedings of IEEE International conference on Computer Science and Automation Engineering (CSAE), Zhangjiajie, China, 25–27 May, 2012, vol. 2, pp. 18–21.

Zinsser, T., Schmidt, J., Niemann, H., 2003. A refined ICP algorithm for robust 3-D correspondence estimation. In: Proceedings of IEEE International Conference on Image Processing, 2003, pp. 695–698.